Title

A multiplatform strategy for the discovery of conventional monoclonal antibodies that inhibit the voltage-gated potassium channel Kv1.3

Journal

mAbs, 10(4)

ISSN

1942-0862

Authors

Bednenko, Janna
Harriman, Rian
Mariën, Lore
et al.

Publication Date

2018-05-19

DOI

10.1080/19420862.2018.1445451

Peer reviewed

A multiplatform strategy for the discovery of conventional monoclonal antibodies that inhibit the voltage-gated potassium channel Kv1.3

Janna Bednenko[a], Rian Harriman[b], Lore Mariën[c], Hai M. Nguyen[d], Alka Agrawal[a], Ashot Papoyan[a], Yelena Bisharyan[a], Joanna Cardarelli[a], Donna Cassidy-Hanley[e], Ted Clark[a,e], Darlene Pedersen[b], Yasmina Abdiche[f], William Harriman[b], Bas van der Woning[c], Hans de Haard[c], Ellen Collarini[b], Heike Wulff[d] and Paul Colussi[a#]

TetraGenetics Inc, Arlington, Massachusetts, USA[a]

Crystal Bioscience, Emeryville, California, USA[b]

argenx, Zwijnaarde, Belgium[c]

Department of Pharmacology, University of California, Davis, California, USA[d]

Department of Immunology and Microbiology, Cornell University, Ithaca, New York, USA[e]

Carterra Inc, Salt Lake City, Utah, USA

Running title: Full-length anti-Kv1.3 monoclonal antibodies

#Address correspondence to Paul Colussi, pcolussi@tetragenetics.com

Abstract

Identifying monoclonal antibodies that block human voltage-gated ion channels (VGICs) is a challenging endeavor exacerbated by difficulties in producing recombinant ion channel proteins in amounts that support drug discovery programs. We have developed a general strategy to address this challenge by combining high-level expression of recombinant VGICs in *Tetrahymena thermophila* with immunization of phylogenetically diverse species and unique screening tools that allow deep-mining for antibodies that could potentially bind functionally important regions of the protein. Using this approach, we targeted human Kv1.3, a voltage-gated potassium channel widely recognized as a therapeutic target for the treatment of a variety of T-cell mediated autoimmune diseases. Recombinant Kv1.3 was used to generate and recover 70 full-length anti-Kv1.3 mAbs from immunized chickens and llamas, of which 10 were able to inhibit Kv1.3 current. Select antibodies were shown to be potent (IC_{50}<10nM) and specific for Kv1.3 over related Kv1 family members, hERG and hNav1.5.

Significance Statement

Despite intense interest from the pharmaceutical industry, progress towards discovery and development of functionally blocking antibodies against human voltage-dependent ion channels has been limited. Using a general strategy that incorporates production of large amounts of correctly folded recombinant protein in the ciliated protozoan, *Tetrahymena*, with immunization of phylogenetically diverse hosts species and deep screening of the immunoglobulin repertoire using novel tools, we have solved this problem for Kv1.3, a potassium efflux channel that plays an important role in activation of effector memory T-cells involved in type 1 diabetes and other autoimmune disorders. With a hit rate of ~14% for functionally blocking antibodies to total antibody binders, this approach may be broadly applicable to the discovery of biologics targeting voltage-dependent channels involved in human disease.

Introduction

Despite the importance of voltage-gated ion channels (VGICs) in human health and disease, the development of therapeutic compounds that can modulate channel activity has proven difficult and been largely restricted to small molecule drugs or peptide toxins that often lack selectivity, have limited bioavailability and/or poor pharmacokinetics. Although monoclonal antibodies (mAbs) with their superior therapeutic profiles could potentially address these issues, discovery programs focused on identifying such antibodies present challenges of their own.

First and foremost, robust platforms for the production of recombinant ion channel proteins have been lacking. This has limited the amount of material available for animal immunizations, as well as the development of antibody screening tools, particularly those that allow deep mining of the immunoglobulin repertoire to identify rare mAbs. Secondly, the high degree of sequence conservation amongst ion channel orthologs, together with the comparatively small extracellular loops on many of these proteins, make ion channels particularly difficult targets for therapeutic antibody development.

To address the first challenge, we have employed the free-living ciliate, *Tetrahymena thermophila*, to overexpress recombinant human VGICs. Genomics studies in *Tetrahymena* have revealed expanded gene families for each of the principal classes of membrane transporters including P-type ATPases, major facilitator superfamily members, ABC transporters, and VGICs (1). Indeed, the *T. thermophila* macronuclear genome sequence predicts more than three times the number of genes for VGICs relative to humans (1). Presumably, these expanded gene families promote *Tetrahymena*'s survival in a continually changing aquatic environment, and are key to physiological responses associated with mating, prey-predator interaction, and food-finding, many of which rely on membrane hyperpolarization and depolarization events that alter cell motility through their effects on ciliary beat (2,3). This core technology platform has allowed us to express mammalian VGICs at levels considerably higher than previously possible in standard mammalian expression systems. This has enabled a

general strategy for the production of antibodies against human ion channels involving 1) antigen formulations incorporating concentrated and highly purified channel proteins; 2) immunization of multiple antibody host species that are phylogenetically diverse; and 3) direct screening of B cells and/or large recombinant antibody libraries with proteins oriented on particle-based solid supports.

As demonstrated here, we have successfully applied this strategy towards the discovery of modulating antibodies against the human voltage-gated K^+ channel, Kv1.3 (hKv1.3), which regulates the membrane potential of both excitable and non-excitable cell types and plays a well-characterized role in regulating Ca^{2+} signaling in activated effector-memory T (T_{EM}) cells (4,5). Up-regulation of Kv1.3 in auto-reactive T_{EM} cells is associated with sites of inflammation in autoimmune disease (5,6), and numerous studies have shown that specific Kv1.3 blockers are effective in a number of animal models of inflammation (5,7-13). Therefore, Kv1.3 is regarded as an attractive target for therapeutic intervention, particularly for type 1 diabetes, multiple sclerosis, psoriasis, and other autoimmune disorders (4,5).

Here we show that recombinant Kv1.3 expressed in *Tetrahymena* traffics to the cell surface, is correctly folded, adopts a native tetrameric conformation and is readily purified from membranes enabling the development of potent immunogens and screening tools. For these initial studies, chickens and llamas were chosen as phylogenetically diverse immune hosts since both have demonstrated success in producing antibodies against highly conserved mammalian proteins (14,15). Using this approach, we identified 70 anti-Kv1.3 mAbs, 10 of which block Kv1.3 currents - an approximate 14% hit rate. Select antibodies demonstrate considerable potency (<10nM) and selectivity (>166 fold) over related channel family members.

RESULTS

Kv1.3 Tetrahymena expression construct design. To maximize expression of human Kv1.3 in *Tetrahymena,* we introduced a codon-optimized version of the *KCNA3* gene driven by a *T. thermophila* cadmium-inducible promoter and linked to a neo2 drug resistance cassette (16) into a high-copy ribosomal DNA vector designated pTRAS1 (Figure 1a). Like its parent plasmid, pD5H8 (17), pTRAS1 retains the ability to form highly amplified, 21 Kb palindromic chromosomes during macronuclear development but contains a wild type rather than paromomycin-resistant version of the 21S ribosomal RNA gene thus favoring retention of the transgene and its linked drug resistance marker that are typically lost through recombination.

Expression and membrane localization of Kv1.3 in T. thermophila. Kv1.3 exists as homotetramer in human T-cells that can be modified by phosphorylation (18). Consistent with this, Western analysis shows that *Tetrahymena* expressed Kv1.3 resolves as two bands, a smaller, 65 kDa band, which is in general agreement with the predicted mass of the Kv1.3 monomer (66 kDa), and a larger 85 kDa band that disappears following treatment with alkaline phosphatase (Figures 1b & c).

Evidence that the recombinant channel assembles into a tetramer was based on staining of fixed cells with K^+ channel peptide toxins. Agitoxin-2 (AgTX-2), Margatoxin (MgTX), and Stichodactyla toxin (ShK) are potent *Shaker* potassium channel blockers derived from the venom of scorpions (AgTX-2; MgTX), and the sea anemone, *Stichodactyla helianthus*, respectively (19-21). These peptide inhibitors bind with high-affinity to the outer vestibule of the tetrameric channel, occlude ion conductance through the pore, and have been used extensively for probing K^+ channel structure (22-27). Fluorescence microscopy showed that both AgTX-2- and ShK-TAMRA bind *Tetrahymena* cells expressing Kv1.3, but not wild-type negative control cells (Figure 1d). At higher magnification, toxins were found to localize at the cell periphery or perinuclear areas enriched in endoplasmic reticulum (ER), suggesting that Kv1.3 assembles into tetramers in the ER before being transported to the cell surface (Figure1d; top right panel).

To ensure binding of the labeled toxins was specific for Kv1.3, cells were co-incubated with 10-fold saturating amounts of competing non-labeled MgTX or Iberiotoxin (IbTX). Iberiotoxin is a potent blocker of large conductance Ca^{2+}-activated K^+ channels derived from *Burthus tamulus* scorpion venom that does not affect voltage-gated potassium channels such as Kv1.3 (28). Figure 1e shows that MgTX but not IbTX competes with both AgTX-2- and ShK-TAMRA binding in Kv1.3 expressing cells. These results confirm that Kv1.3 traffics to the *Tetrahymena* cell surface as a correctly assembled tetramer.

***Kv1.3 purification, reconstitution, and characterization*.** Kv1.3 containing a C-terminal His tag was extracted from *Tetrahymena* membranes with the detergent FC12 after pre-treatment with digitonin and purified by nickel affinity chromatography. Psora-4, a specific small molecule Kv1.3 inhibitor was maintained in extraction and purification buffers to stabilize the channel and generally resulted in increased yields. The majority of the purified protein resolved as a doublet of ~65 kDa and ~85 kDa on SDS-PAGE, with additional Coomassie stainable material being present at higher (>250 kDa) molecular mass (Figure 2a). Both the doublet and higher mass species were confirmed to consist of Kv1.3 by anti-Kv1.3 Western analysis and mass spectroscopy analysis. Multiple purifications (n=7) resulted in a range of recovery of purified protein between 0.5-3 mg/L and an average recovery of 1.3 mg Kv1.3 per liter of culture. Purified Kv1.3 was either reconstituted into phosphatidylcholine-based proteoliposomes for long-term storage (Figure 2a) or adhered to magnetic beads via the C-terminal His tag as described in methods (Figure 2c,d & e).

Three separate batches of Kv1.3 proteoliposomes were analyzed in independent experiments to estimate binding affinity constants using fluorescence polarization (29-31). Fluorescein 6-carbonyl (FAM)-labeled ShK (FAM-ShK, 3 nM) was added to increasing amounts of Kv1.3-containing proteoliposomes in the absence or presence of a 50-100-fold excess of competing MgTx or IbTx. Figure 2b is a representative experiment showing that total FAM-ShK binding increased with increasing amounts of protein and that MgTx, but not IbTx, competed

with ShK binding (top panel). Specific binding curves (Figure 2b, bottom panel) were used to determine an average binding affinity (K_d) of 11.5 nM +/- 3.4 nM (*n*=3), approximately 200-fold lower than the IC_{50} (52 pM) reported for FAM-ShK using patch clamp electrophysiology (27).

Generation of anti-Kv1.3 antibodies. Two chickens were immunized with Kv1.3 proteoliposomes (with DNA/LPS adjuvant) as described in Methods. One chicken (19724) demonstrated a specific titer at week 6 and was chosen for further study. Anti-Kv1.3 antibodies were identified in Gel Encapsulated Microenvironment (GEM) assays using splenocytes recovered from chicken 19724 and antigen reporters (that is, screening tools) comprised of either polystyrene beads coated with Kv1.3 proteoliposomes; Kv1.3 magnetic beads containing right side out, oriented Kv1.3 protein (Figure 2c, d & e); or, Kv1.3-expressing *Tetrahymena* cells. Antibodies were recovered from each screen generating 51 sequence unique scFv-Fc clones in total (summarized in Table 1). Each antibody bound Kv1.3 by ELISA, however, clone ch_p1E6 demonstrated significantly less activity compared to other clones and ch_p1F8 also bound the non-related ion channel (NRIC) proteoliposomes control (the binding of a subset of these antibodies is shown in Figure 3a). MAbs recovered from GEM screens incorporating Kv1.3 proteoliposomes or magnetic beads were additionally tested for their ability to bind Jurkat cells via flow cytometry. Jurkat cells are a human leukemia T-cell line that has been reported to express approximately 200 active Kv1.3 ion channels per cell (32). Of 41 antibodies tested, Jurkat cell binding was detected with 6 antibodies (ch_p1A11, ch_p1H7, ch_p1D8, ch_p1E6, ch_p2A3 and ch_p2G9) comprising a range of median fluorescence intensity of 1157 to 9401 compared to an average MFI of 198 +/- 41 (*n*=35) for all other antibodies analyzed.

To generate antibodies in llamas, four animals were immunized and boosted with plasmid DNA encoding Kv1.3 six times and were additionally boosted with Kv1.3 proteoliposomes twice. Kv1.3-specific immune responses were measured for Kv1.3 proteoliposomes versus NRIC proteoliposomes. Three out of four llamas showed an immune response against Kv1.3 proteoliposomes, but also to irrelevant proteoliposomes. Nevertheless,

scFv libraries were constructed for two llamas (Armello and Lisandro) that exhibited the strongest responses against Kv1.3 proteoliposomes. Two phage libraries were created for each llama, comprising combinations of the immunoglobulin heavy chain repertoire and either the κ light chain, or λ light chain repertoires, resulting in library sizes of approximately 3-8 x 10^8 clones. Phage panning was performed on Kv1.3 magnetic beads. After two rounds of phage selections, an enrichment of 10-fold for library Armello κ, 18-fold for Armello λ, 43-fold for Lisandro κ and 100-fold for Lisandro λ over NRIC magnetic beads was achieved. Individual soluble scFv fragments in periplasmic fractions were screened on mesoscale for specific binding to Kv1.3 proteoliposomes. Only a limited screening of 36 clones per library was performed, nevertheless 48 out of the 144 screened clones displayed specific binding. Sequencing of the VH and VL regions of these specific clones showed that they could be divided into 19 different VH families based on VH CDR3 sequence length and similarity. The clones derived from the Armello κ scFv library consisted of 5 VH families, from Armello λ of 3 VH families, from Lisandro κ of 9 VH families and from Lisandro λ of 3 VH families. Nineteen clones representing the best performing clone on mesoscale of each different family were selected to be re-cloned as scFv-Fc fusion proteins. After transfection, production in HEK293E cells, and protein A purification, a new specificity screen on mesoscale was initiated. For all scFv-Fc molecules representing these 19 different VH families, specific binding to Kv1.3 could be reconfirmed (the binding of a subset of these antibodies is shown in Figure 3b).

Identification of functionally inhibiting anti-Kv1.3 antibodies. Purified scFv-Fc anti-Kv1.3 antibody clones were tested by whole-cell patch-clamp at a single concentration (400 nM) for inhibition of human Kv1.3 channels transiently expressed in L929 mouse fibroblast cells. Nine chicken mAbs and one llama mAb were identified as inhibiting Kv1.3 activity (Figure 4a & b). Each functional antibody was derived from antibody screens incorporating either Kv1.3 proteoliposomes and/or magnetic beads (Table 1) and blocked between 44-82% of Kv1.3 currents (Table 2) within 600 seconds of application (Figure 4d). None of the antibodies tested,

chicken or llama, under the assay conditions used, displayed agonist activity towards the Kv1.3 channel. Interestingly, while not all of the functional chicken antibodies bound Jurkat cells as detected by flow cytometry, each of those that did were functionally active.

Based on the relative inhibition of current at 400nM the most potent chicken antibody (ch_p1E6) and the llama L1A3 antibody were characterized further. Dose response analysis determined IC_{50} concentrations for ch_p1E6 and L1A3 as 6 and 109nM, respectively (Figure 5a & b). Selectivity for each of the antibodies was assessed on related Kv1.x family members (Kv1.1, Kv1.2, Kv1.5), hERG (Kv11.1) and Nav1.5. At 1μM neither antibody inhibited activity more than 5% for any of the channels tested (Figure 5c & Table 3) indicating that the fold selectivity for Kv1.3 is, at minimum, greater than 166-fold for ch_p1E6 and 9-fold for L1A3.

Epitope binning analysis. Owing to the large recovery of functional antibodies, particularly from chickens, we performed an epitope binning analysis to gain an understanding of the diversity of epitopes recognized by the anti-Kv1.3 antibodies and to determine if there was a correlation between functional activity and epitope bins. Thirty-six chicken mAbs including eight of the nine functional antibodies (clone ch_p1E6 was excluded-see below) and the llama L1A3 antibody were analyzed by array-based SPR imaging. A heat map of the binning analysis indicates that antibodies can be divided into at least 5 epitope bins based on their ability to block competing antibody binding to the Kv1.3 antigen (Figure 6a). A network plot (Figure 6b) highlights the fact that a majority (56.7%) of the antibodies fall into one bin (Bin 1) that includes 7 of the 9 functional antibodies tested. Bin 2 contains 23% of the antibodies tested and includes 1 functional antibody (ch_p1F8), whereas Bins 3 and 4 contain 13.5 and 5.4% of antibodies tested, respectively, and do not contain any functional antibodies. Binding to Kv1.3 by clone ch_p1D8 was not blocked by any other antibodies tested and therefore was assigned its own epitope bin (Bin 5). No obvious correlation was noted between epitope bin assignment and antibodies that in addition to functionally inhibiting Kv1.3 activity also bound Jurkat cells.

Clone ch_p1E6 binding to Kv1.3 in the SPR format was insufficient to enable analysis - a result most likely related to the poor binding of this antibody to purified antigen in ELISAs. However, its potency in blocking mammalian expressed Kv1.3 and ability to bind Jurkat cells suggests that ch_p1E6 effectively binds native Kv1.3 in mammalian cells at an epitope that is partially lost during purification of the channel or its preparation for ELISA and therefore represents a separate bin (i.e. Bin 6).

DISCUSSION

A number of groups have successfully generated anti-Kv1.3 immunoglobulins that inhibit channel activity, including polyclonal antibodies generated in rabbits (33), heavy chain only VHH nanobodies in llamas (US Patent Application 20170137512), and engineered cowbodies that incorporate inhibitory Kv1.3 toxins into the ultralong CDR that are characteristic of these antibodies (34). However, to our knowledge, this study describes the first set of conventional mAbs capable of blocking the activity of human Kv1.3. To achieve this, we applied a general strategy designed to mitigate several of the challenges associated with the production of functional antibodies against human VGICs. Importantly, we used *Tetrahymena thermophila* as an expression platform to generate sufficient quantities of recombinant Kv1.3 to support the development of different types of immunogens and antibody screening tools. While previous studies have suggested the utility of this system for the production of recombinant membrane proteins in general (1), the present work clearly underscores this for voltage-gated ion channels in particular. While the choice of a K^+-selective channel for these initial studies was based partially on the fact that the vast majority (308 of 332) of annotated VGIC genes in *Tetrahymena* predict K^+-selective channels (1), recent studies have shown this system works equally well for the production of a wide range of other human channels.

Localization studies with fluorescently tagged peptide toxins suggest that recombinant Kv1.3 produced in these cells can assemble into homotetramers and traffic to the membrane surface (Figure 1). However, Kv1.3 was found to be essentially insoluble in the absence of digitonin, with FC12 being the most efficient detergent tested for ion channel extraction. The affinity of Kv1.3 purified under these conditions was approximately 200-fold lower for ShK than that reported for Kv1.3 expressed in mammalian cells. The reduced affinity of the purified channel is not entirely surprising and may be attributable to a number of factors including subtle changes in protein folding, which may, in turn, be due to altered post-translational modifications and/or the artificial lipid environment of the purified channel. Nevertheless, the immunogen and

antibody screening formulations described here were sufficient to generate and identify functionally inhibiting anti-Kv1.3 antibodies thus confirming the utility of *Tetrahymena* for the expression of native or near-native mammalian channel proteins.

Both chickens and llamas were used as phylogenetically distinct species for immunization. In all 70 anti-Kv1.3 antibodies were identified (51 from chickens and 19 from llamas). Of those, 10 were capable of blocking Kv1.3 current - an approximately 14% discovery success rate for functional antibodies. Further analysis of a select chicken antibody, ch_p1E6, and the functional L1A3 llama antibody, revealed potencies of 6 nM and 109 nM, respectively, while neither showed any appreciable activity on related K^+ or Nav1.5 channels at a concentration of 1 μM thus confirming that conventional mAbs can selectively and potently inhibit Kv1.3 function with IC_{50}s in the single-digit nM range.

A majority (90%) of the blockers were derived from chickens while a single functional antibody was isolated from phage libraries constructed from immunized llamas. One reason for the higher rate of recovery of functional chicken antibodies may be due to the overall sequence divergence between Kv1.3 in humans, chickens and llamas. Human Kv1.3 shares 97.5% and 97.7% identity with mouse and llama Kv1.3, respectively, but only 83% identity with chicken Kv1.3. Moreover, analysis of the three Kv1.3 extracellular cellular domains (ECD) where antibodies would be presumed to exert their effect, reveals further divergence with the human sequence, with the first extracellular loop showing 85.7%, 80.95%, and 52.5% identity with mouse, llama and chicken sequences, respectively (summarized in Table 4).

A further, and perhaps critical consideration in our overall strategy was to avoid hybridoma-based antibody generation and screening methods to mitigate the effects of non-efficient fusion events and loss of rare B cell clones leading to a decrease in diversity of the screenable immune repertoire (35). In the current study, functional antibodies were identified in screens of B cells (chicken mAbs) or from phage display libraries (llama mAbs) using either Kv1.3 proteoliposomes applied to a solid support (polystyrene beads) or from formulations

containing Kv1.3 oriented on magnetic beads directly via an engineered C-terminal tag. Seven of nine of the functional chicken mAbs were isolated using Kv1.3 proteoliposomes adhered to polystyrene beads suggesting that this formulation was particularly efficient for recovering functional mAbs. Interestingly, llama phage display libraries were panned with Kv1.3 magnetic beads alone, therefore, the role of phylogenetic diversity notwithstanding, altering the screening methodology to incorporate Kv1.3 proteoliposomes could potentially increase the recovery of functional antibodies from these phage libraries. Furthermore, given the fact that chicken mAbs capable of recognizing the native channel expressed in Jurkat cells also blocked channel activity, a direct screen or potentially another round of phage selection on these cells could have delivered a higher frequency of functional llama antibodies.

A binning analysis of the chicken anti-Kv1.3 mAbs identified 5 epitope bins with a majority of the antibodies, including 6 of the 8 functional antibodies tested, segregating into one bin. Furthermore, the llama L1A3 mAb, used as a reference in the analysis, segregated to the same bin suggesting a single Kv1.3 epitope was responsible for generating a majority of the functional antibodies in both platforms.

Significant progress is being made in the clinic targeting Kv1.3 with the highly potent venom peptide analog ShK-186 for the treatment of plaque psoriasis (36). In subsequent studies it will be of considerable interest to determine if one or more of the inhibitory mAbs described here exhibit similar efficacy and additionally display the benefits of long immunoglobulin half-life in a clinical setting. We hypothesize that a stable and potent anti-Kv1.3 mAb may offer significant advantages in enabling a therapeutic intervention that halts the autoimmune cascade in a number of serious human diseases including type 1 diabetes and multiple sclerosis.

METHODS

Cells and reagents. *T. thermophila* strains B2086 (*mat1-2/mat1-2* [*mat1-2*; II) and CU428 (*mpr1-1/mpr1-1* [*MPR1*; mp-s, VII]) were obtained from the *Tetrahymena* stock center (Cornell University). Restriction endonucleases were from New England Biolabs. Anti-FLAG antibody was from Thermo Fisher Scientific (#MA1-91878), anti-C-terminal His antibody was from Life Technologies (#R93025), anti-Kv1.3 antibody was from Alomone (#AGP-005). Anti-mouse HRP-conjugated antibody was from Bio-Rad Laboratories (#1706516) and anti-guinea pig HRP-conjugated antibody was from Life Technologies (#A18775). Kv1.3 toxins, Margatoxin (MgTX, #STM-325), Agitoxin-2-TAMRA (AgTX-2-TAMRA, #RTA-420-T) and Iberiotoxin (IbTX, #STI-400) were from Alomone. ShK-TAMRA was from Smartox (#SAT001-00100) and FAM-ShK was obtained from Bachem (#H-6088). *T. thermophila* growth media reagents, protease peptone (#9000270), yeast extract (#9000726), glucose (#VWRBK876) were from VWR. $FeCl_3$ was from ThermoFisher Scientific (#ICN15349980). Psora-4 was from Sigma (#P9872).

Expression construct design and cloning. A synthetic gene encoding the human *KCNA3* gene (accession number P22001.3) modified with an in-frame C-terminal dual FLAG-10XHis (DYKDDDDKHHHHHHHHHH) affinity tag was codon-optimized for expression in *Tetrahymena* and synthesized by GenScript. The synthetic gene was cloned into a somatic expression vector, pTIEV5, via PacI and SacI restriction sites engineered into the 5' and 3' ends of the synthetic gene, respectively. Transcription of the transgene was under the control of the inducible *Tetrahymena* metallothionein-5 (MTT5) gene promoter. The expression construct comprising MTT5 promoter, Kv1.3 gene, MTT1 terminator and a neomycin resistance cassette was transferred as a single NotI fragment into a high-copy rDNA vector, pTRAS1.

Generation of Kv1.3 expression strains. The Kv1.3 pTRAS expression vector was introduced into conjugating B2086 and CU428 *T. thermophila* strains by biolistic transformation as described previously (37). Briefly, 20 μl of M17 tungsten beads (Bio-Rad Laboratories) were

coated with 8 μg of expression vector DNA. Transformations were carried out using a Biolistic PDS-1000/He Particle Delivery System (Bio-Rad Laboratories) approximately 10 hours following induction of conjugation. Following particle bombardment and recovery in NEFF medium (0.25% proteose peptone, 0.25% yeast extract, 0.55% glucose, 33 mM $FeCl_3$) at 30°C for 18 h, cells were supplemented with paramomycin (100 μg/ml), aliquoted into 96-well microplates and incubated for 3-4 days at 30°C. Wells containing paromomycin-resistant cells were identified and transferred to stock tubes. To identify Kv1.3 expressing cell lines, drug-resistant clones were grown in 3 ml cultures to a cell density of at least 5 x 10^5 cells/ml and Kv1.3 expression was induced by the addition of 2 μg/ml $CdCl_2$. Cells were harvested at 6 h post-induction and stored at -20°C. Cells expressing Kv1.3 were identified by Western blot analysis using anti-Kv1.3 and/or anti-tag antibodies. To establish clonal cell lines, single cells were isolated from Kv1.3-expressing stock tubes into drops of NEFF media containing 100 μg/ml paromomycin. Single cell clones were transferred to stock tubes and the best expressing cell lines were identified by Western blot analysis.

Kv1.3 localization. To determine cellular localization, *T. thermophila* wild-type (CU428) and Kv1.3 expressing cells were fixed with 4% paraformaldehyde for 30 min. *Tetrahymena* cells fixed under these conditions become permeable and allow passage of reagents through the plasma membrane. Cells were incubated in the presence of either 10 nM ShK-TAMRA or 10 nM Agitoxin-2-TAMRA for 30 min. Cells were washed three times in PBS buffer and visualized by fluorescence confocal microscopy using an SP5 Leica laser scanning confocal microscope with a 63X oil objective lens. To investigate specific-binding of Kv1.3 toxins, cells were co-incubated with 10 nM ShK-TAMRA and saturating amounts (100 nM) of either Margatoxin (ShK competitor) or Iberiotoxin (non-competing toxin).

Kv1.3 Purification. Cells expressing Kv1.3 were resuspended in ice-cold 1x PBS buffer and disrupted by a single pass through a M-110P Microfluidizer (Microfluidics) at 4,000 Psi.

Disrupted cell membranes were collected by centrifugation at 100,000 x g for 1h at 4°C, resuspended in ice-cold PBS and stored at -80°C. Crude membrane pellets were resuspended in TKG buffer (30 mM Tris HCl pH 7.4, 300 mM KCl, 10% glycerol) containing 1% n-dodecyl-b-D-maltoside (DDM, Anatrace, #D310), 0.2 μg/ml Psora-4, 0.25% phosphatidylcholine (Sigma-Aldrich) and protease inhibitors (Roche #11836170001, cOmplete protease inhibitors, EDTA-free, 1 mini-tablet per 10 ml buffer) and incubated 1 h at 4°C to allow extraction of *Tetrahymena* membrane proteins (Kv1.3 is not extracted under these conditions). Pre-extracted membranes were harvested by centrifugation at 100,000 x g for 1h at 4°C and then resuspended in TKG buffer containing 0.02% digitonin, 0.2 μg/ml Psora-4, protease inhibitors and incubated for 1h at 4°C. An equal volume of extraction buffer (TKG containing 2% FOS-choline 12, 10 mM EDTA, 0.2 μg/ml Psora-4, 0.5% phosphatidylcholine) was added dropwise and the suspension was incubated for 1h at 4°C. The suspension was centrifuged (100,000 x g) for 1h at 4°C and a cleared lysate collected and supplemented with 6 mM $MgCl_2$ and 50 mM Imidazole. Kv1.3 was purified using Ni Sepharose 6 Fast Flow (GE Healthcare) resin. Bound protein was washed first in TKG buffer containing 0.1% DDM, 0.2 μg/ml Psora-4, 0.025% phopshatidylcholine and 50 mM imidazole and then in TKG buffer containing 0.025% DDM, 0.2 μg/ml Psora-4, 0.00625% phopshatidylcholine and 200 mM imidazole. Kv1.3 was eluted in TKG buffer containing 0.025% DDM, 0.2 μg/ml Psora-4, 0.00625% phopshatidylcholine and 750 mM imidazole and dialysed in the same buffer lacking imidazole. Protein was concentrated in an Amicon stirred cell concentrator fitted with an Ultracel® 100 kDa ultrafiltration disk (Millipore, # PLHK02510) under a stream of nitrogen.

Reconstitution of purified Kv1.3 into liposomes. L-α-phosphatidylcholine (Anatrace, #131601P) was dried down under nitrogen and resuspended in buffer containing 20 mM Tris-Cl, 100 mM KCl, pH7.4 to a final concentration of 40 mg/ml. Lipids were rehydrated for 2 h at room temperature with 30 second bursts in a sonicating water bath every 10-15 min. Lipids were

further sonicated for 5 min, frozen in liquid N_2 and thawed in a 30°C water bath. This process was repeated 2 times. Liposomes were clarified with an Avanti mini-extruder fitted with a 0.1 micron filter. Purified protein (0.5-1.0 mg/ml) was added to liposomes at a ratio of 3:1 and incubated for 10 min at RT followed by sonication in a water bath for 10 min. The protein-liposome mix was then added to 150 mg hydrated Bio-Beads SM2 (Bio-Rad Laboratories, #152-8920) per ml of liposome mix and incubated overnight at 4°C. Proteoliposomes were separated from Bio-Beads using a pulled Pasteur pipette, sonicated in a water bath for 5 min, snap frozen in liquid N_2 and stored at -80°C.

Fluorescence Polarization Ligand Binding Analysis. Two-fold serial dilutions of Kv1.3 proteoliposomes were mixed with 3 nM FAM-ShK in duplicate in 20 mM Tris pH 7.4, 2.5 mM KCl, 0.1% BSA, in the presence or absence of a 50-100-fold excess of MgTx (ShK competitor) or IbTx (irrelevant ligand), for 1 h at room temperature. Assays were carried out in 150 μl volumes per well in flat bottom, non-binding surface 96-well black plates (Corning, #3991). Fluorescence anisotropy readings were taken using a Tecan Infinite M1000 Pro at an excitation wavelength of 470 nm and an emission wavelength of 535 nm. The specific binding (in the presence of MgTx) was determined and used to calculate the K_d by nonlinear regression using GraphPad Prism (GraphPad Software, La Jolla, CA) to the equation (which assumes protein depletion):

$$A = A_f + (A_b - A_f) \times \frac{(L_T + K_d + R_T) - \sqrt{(-L_T - K_d - R_T)^2 - 4L_T R_T}}{2L_T}$$

where

A = anisotropy (measured)

R_T = total protein concentration (known)

L_T = fluorescent ligand concentration (3 nM)

A_f = anisotropy of free ligand (calculated)

A_b = anisotropy of bound ligand (calculated)

K_d = dissociation constant (calculated)

Kv1.3 Magnetic Beads. Purified Kv1.3 was incubated with a slurry of magnetic His tag Dynabeads® (Thermo Fisher Scientific, #10103D) pre-equilibrated in buffer A (30 mM Tris-Cl, 300 mM KCl, 10% glycerol, 0.025% DDM, 0.00625% phosphatidylcholine, pH 7.4) for 2 h at 4°C. The Kv1.3 to bead ratio was approximately 1 mg protein to 1 ml slurry. Beads were washed with buffer A, mixed with rehydrated lipids (10 mg/ml egg L-α-phosphatidylcholine [Anatrace, #131601P], +/- 0.05 mg/ml rhodamine-conjugated 1,2-dioleoyl-sn-glycero-3-phosphoethanolamine [Anatrace, 810150P]) and incubated for 15 minutes at 4°C. The magnetic bead lipid mixture was incubated in a sonicating water bath for 10 minutes, then transferred to a new glass vial containing 200 mg hydrated Bio-Beads and rotated overnight at 4°C. Magnetic beads were separated from Bio-Beads with a pulled Pasteur pipette, washed and resuspended in buffer B (20 mM Tris-Cl, 100 mM KCl, pH 7.4).

Immunizations and antibody screens.

A. Chicken

Immunization. Two female 6-wk old White Leghorn chickens were immunized intramuscularly initially with 112 μg purified recombinant Kv1.3 reconstituted into proteoliposomes. Boosts continued every other week using 85 μg, 112 μg, 280 μg and 390 μg, with a final IV boost of 280 μg. Fifteen micrograms bacterial plasmid DNA and 10 ul of E. coli Lipopolysaccharide (LPS, Alexis #581-012-L002) were added as adjuvant to the liposomes in a final volume of 0.5 ml for the 2nd, 3rd and 4th boosts, and Lipid A was also added at the 4th boost. The immunization protocol was IACUC approved. During the course of the immunizations chickens were monitored for signs of discomfort and illness; neither bird showed any sign of either. Titers were determined by ELISA: 96-well plates were coated overnight at 4°C with 2 μg/ml Kv1.3 or

proteoliposomes containing a non-related ion channel (NRIC), washed 3 times with PBS, and blocked with 3% milk in PBS (PBSM) for 1 h. Dilutions of the sera were added in PBSM and incubated for 1 h, then the plate was washed 3 times with PBS, and anti-chicken IgY-HRP (Sigma, #A9046) was added in PBSM for 1 h. The plate was washed 3 times with PBSM, developed using TMB (Thermo Fisher Scientific, #2023) for 10 min, quenched with 1 N HCl, and read at 450 nm. Final titer reached 1:250 for bird 19718, and greater than 1:30,000 for bird 19724.

Screening splenic B cells for Kv1.3 reactive antibodies. Splenocytes were recovered from bird 19724 four days after the final antigen IV boost and incorporated into Gel Encapsulated Microenvironments (GEMs) according to Izquierdo *et al.* (38). GEMs were prepared using three strategies.

1. *Polystyrene bead reporters:* 5 µm polystyrene beads (Thermo Fisher Scientific, #A37306) were coated with Kv1.3 or NRIC proteoliposomes at a 5x mass ratio overnight. NRIC was coated onto beads dyed with coumarin to render them blue by fluorescence. Beads were washed and blocked with PBSM. The two beads were used in GEMS with chicken splenocytes, the blue NRIC bead serving as a specificity control.

2. *Magnetic Dynabead particles*: Kv1.3 magnetic beads were prepared as described above. The magnetic particles were incorporated into GEMS with chicken splenocytes.

3. *Tetrahymena cells*: *Tetrahymena* expressing Kv.1.3 were fixed with 4% paraformaldehyde, washed, and incorporated into GEMS with chicken splenocytes.

Cloning and Expression of Kv1.3 recombinant antibodies. As described in Izquierdo *et al.* (38), chicken VH and VL gene segments were PCR amplified from individual positive B cells identified in the GEM assay, cloned into a scFv-Fc expression vector (human Fc), and transiently expressed in Expi293 cells grown in Expi293 Expression Medium using

Expifectamine (Thermo Fisher Scientific, #A14524), in 96-well format. Supernatants were tested for binding by ELISA, as described above, using anti-human-Fc-HRP (VWR #RL609-4303) secondary antibody. Unique clones were re-transfected in a 2 ml culture to confirm binding and for further evaluation. Supernatant antibody concentrations were quantitated by sandwich ELISA using anti-human-Fc and a scFv-Fc control. To purify antibodies for electrophysiology, 40 ml cultures were used for transfections, and antibody purified using Protein G Agarose (Thermo Fisher Scientific, #20399B) according to the manufacturer's protocol.

Flow cytometry: Jurkat cells (clone E6, ATCC) were grown in RPMI (Thermo Fisher Scientific, #450000-404) supplemented with 10% fetal calf serum (Hyclone, #SH30071.03) and Glutamax (Thermo Fisher Scientific, #35050061). Cells (1.5e5 /well) were incubated at 4°C for 1h with 10 μg/ml of each antibody diluted in PBS/1% BSA/0.1% sodium azide (FACS buffer), washed 2 times with FACS buffer, incubated with anti-human IgG-PE (Jackson Immunoresearch, #109-115-098) at 5 μg/ml at 4°C for 1h, washed 2 times with FACS buffer, resuspended in FACS buffer and read on an Attune Cytometer (Thermo Fisher Scientific).

B. Llama

Llama immunization and library construction: Llama immunization, peripheral blood lymphocytes (PBLs) isolation, RNA extraction and the construction of scFv libraries were performed as described previously (39). All llamas used in this study were farmed outdoors in the Ardèche region of France according to French animal welfare legislation. Animal handling included immunization by intramuscular injection and peripheral blood collection. As a rule, experimental use of llamas is limited to a single immunization protocol; following the last blood drawing, animals are employed for recreational use. Within the framework of the guidelines four llamas were immunized six times biweekly with 2 mg/ml plasmid DNA encoding human Kv1.3 under

control of a CMV promoter. A boost with 50 μg Kv1.3 proteoliposomes was given two times biweekly. Before the start and a week after completion of the immunizations, serum was prepared from 10 ml blood in EDTA tubes. PBLs were isolated from 400 ml blood collected five days after the last immunization, and RNA extraction and cDNA amplification was done as formerly described (40). Immune responses were measured on pre- and post-immunization serum samples by mesoscale against both Kv1.3 and NRIC proteoliposomes, coated at 1 μg/ml. Detection of serum titrations was performed using a mouse anti-llama IgG-CH1 (in-house antibody) and an anti-mouse sulpho antibody (MSD, #R32AC-5). Subsequently, scFv libraries were made for two of the four immunized llamas as previously described (39). In brief, VH, Vκ and Vλ libraries were independently constructed into the pSc vector, which was derived from the pCB3 phagemid vector. Re-cloning the light chain libraries in the VH library was performed, to obtain the combinatorial κ and λ library for each llama.

Phage selection: Phage production and selection were performed according to standard protocols (39,41). Phages expressing scFv fragments were allowed to bind for 2 h at 4°C to rotating Kv1.3 or NRIC magnetic beads. Washing steps were performed using PBS containing 0.05% Tween and elution of phages was done by using 10 mg/ml trypsin (Sigma-Aldrich, #T1426). Two rounds of selection were carried out using 10 μg Kv1.3 magnetic beads and 20 μl input phages in the first round and respectively 2 μg and 2 μl in the second round to enrich for phages expressing scFv fragments binding specifically to Kv1.3. The Kv1.3-binding clones were isolated as individual colonies and expression of soluble scFv fragments in the periplasmic space was induced using isopropyl β-D-1 thiogalactopyranoside (Thermo Fisher Scientific, #R0391).

Screening binding assays: Individual soluble scFv fragments in periplasmic fractions were screened for binding to 1 μg/ml Kv1.3 and NRIC proteoliposomes using mesoscale. The

detection was carried out using mouse anti-myc antibody 9E10 (Bethyl Laboratories, #A190-105P) and an anti-mouse sulpho antibody. The cut-off ratio for binding to Kv1.3 over NRIC proteoliposomes was set to 2. The positive clones were sent for sequencing (LGC Genomics) to determine the number of families based on VH CDR3 sequence length and similarity (42). VH and VL sequences from selected clones were re-cloned in the scFv-Fc backbone where the scFv was fused to the hinge-CH2-CH3 domain of a human IgG1. Transfection, production in HEK293E cells (ATCC, #CRL-10852) and protein A purification were performed as previously described (40). scFv-Fc screening using a 1/10 dilution series starting from 1 μg/ml was carried out to confirm binding to Kv1.3. By mesoscale, screening for binding to Kv1.3 and irrelevant proteoliposomes, coated at 1 μg/ml was done using an anti-human sulpho detection antibody (MSD, #R32AJ-5). As a positive control, a polyclonal anti-Kv1.3-biotin antibody was also assessed (Alomone, #APC-101-B).

Antibody screening and potency (IC_{50}). Antibodies were tested on human Kv1.3 channels that were transiently expressed in L929 fibroblast cells (ATCC). Stable expression and sources of the mKv1.1, rKv1.2, hKv1.5, hNav1.5 and hKv11.1 (hERG) channels were described previously (43,44). Cells were maintained in a culture medium of Dulbecco's modified Eagle's medium (DMEM) supplemented with L-glutamine and 10% heat-inactivated fetal calf serum in a humidified, 5% CO_2 incubator at 37°C. For transient expression, hKv1.3 cells were transfected in conjunction with pEGFP, using FuGENE® 6 transfection reagent (Promega, #E2691) in OptiMEM reduced serum medium (Life Technologies, #31985088), for identification of transfected cells under the epifluorescence microscope after 24 to 72h post-transfection. All cells were detached by trypsinization and plated on cover-slips coated with poly-L-lysine for whole-cell patch-clamp recording using the EPC-10 HEKA amplifier. All currents were recorded in normal Ringer' solution containing (in mM): 160 NaCl, 4.5 KCl, 2 $CaCl_2$, 1 $MgCl_2$, 10 HEPES (adjusted to pH 7.4 and 290–310 mOsm). Patch pipettes were pulled from soda lime glass

(micro-hematocrit tubes, Kimble Chase, Rochester, NY) to resistances of 2-3 MΩ and filled with an internal pipette solution containing (in mM): 145 KF, 2 $MgCl_2$, 10 HEPES, 10 EGTA (pH 7.2, 290–310 mOsm) for Kv1.1, Kv1.2, Kv1.3 and Kv1.5 recordings; 120 KCl, 10 HEPES, 4 Na_2ATP, 10 EGTA, 5.374 $CaCl_2$, 1.75 $MgCl_2$ (pH 7.2, 290-310 mOsm) for hERG recordings; and 10 NaF, 110 CsF, 20 CsCl, 2 ethylene glycol tetraacetic acid, 10 HEPES (pH 7.35, 300 mOsm) for Nav1.5 recordings. Outward K^+ currents were elicited using repeated 200-ms long depolarizing pulses to 40 mV with a 30-s interpulse interval for Kv1.3 and a 10-s interpulse interval for Kv1.1, Kv1.2 and Kv1.5. hERG currents were recorded with a two-step pulse from -80 mV first to 20 mV for 3 seconds and then to -50 mV for 2 seconds. Inward Na+ currents were elicited by 50-ms pulse to 0 mV from -90 mV applied every 10-s. Cell capacitance, a direct measurement of cell surface area, and access resistance were continuously monitored during recordings to ensure minimal current rundown. Test antibody solutions were freshly made in normal Ringer's solution immediately prior to bath perfusion, which was performed only once currents had stabilized from the preceding control condition or testing dose. IC_{50} values were determined by fitting the calculated percentage of current blocked to a Hill equation using the software Origin 9.0 (*OriginLab*). Data are presented as means ± standard deviations.

Epitope binning. A panel of 36 sequence unique anti-Kv1.3 chicken mAbs (scFv-Fc constructs) supplied as crude transfectant supernatants, was epitope binned using a "premix" assay format by array-based SPR imaging (Array SPRi) as described previously (45). In addition, select clones were also supplied in purified form (1D8, 1H7, 2A3, and 2G9) along with a functionally inhibiting llama anti-Kv1.3 reference antibody (L1A3) and coupled as a 48-spot array. The analysis was performed at 25°C on a Xantec CMD 200 M sensor chip and in a running buffer of 10 mM Hepes pH7.4, 150 mM NaCl, 3 mM EDTA, 0.05% Tween-20 (HBS-EP+) with 1 g/l BSA using premixed samples containing 33 nM Kv1.3 and 480 nM antibody (in binding sites) and regenerating each binding cycle with 75 mM phosphoric acid.

Acknowledgements

Work at TetraGenetics was funded in part by JDRF T1D Fund (www.t1dfund.org)

Author Contributions

J. Bednenko generated Kv1.3 expressing Tetrahymena strains and purified recombinant Kv1.3 and contributed to manuscript writing; R. Harriman performed GEM assays, antibody cloning and initial characterization of chicken antibodies; L. Mariën was involved in the conception and design of llama antibody production, collection and assembly of data, data analysis and interpretation and manuscript writing; H. Nguyen performed electrophysiological experiments and contributed to experimental design, data analysis and interpretation, and manuscript writing; A. Agrawal performed ligand binding analysis and contributed to manuscript writing; A. Papoyan generated Tetrahymena Kv1.3 expression constructs; Y. Bisharyan performed Tetrahymena fluorescence microscopy; J. Cardarelli optimized expression of Kv1.3 in Tetrahymena for purifications; D. Cassidy-Hanley contributed to the conception and design of the Tetrahymena rDNA expression vector pTRAS1; T. Clark contributed to the conception and design of expreriments involving Kv1.3 expression in Tetrahymena and to manuscript writing; D. Pederson performed immunizations and determined sera titers in chickens; Y. Abdiche carried out epitope binning analysis and contributed to manuscript writing; W. Harriman and E. Collarini were involved in the conception and design of chicken antibody production, data analysis and interpretation and manuscript writing; B. van der Woning was involved in the conception and design of llama antibody production, collection and assembly of data, data analysis and interpretation and manuscript writing; H. de Haard was involved in the conception and design of llama antibody production, data analysis and interpretation, manuscript writing and approval; H. Wulff contributed to electrophysiology experimental design, data analysis and interpretation and

manuscript writing; P. Colussi contributed to the conception and design of each aspect of the described work, data analysis and interpretation and manuscript writing.

Competing Financial Interests

The following authors indicated a financial or other interest that is relevant to matters in this article: J. Bednenko, A. Agrawal, A. Papoyan, Y. Bisharyan, J. Cardarelli, T. Clark and P. Colussi are employees of TetraGenetics Inc; R. Harriman, D. Pedersen, W. Harriman, and E. Collarini are emplyees of Crystal Bioscience; L. Mariën, B. van der Woning and H. de Haard are employees of argenx and H. deHaard has ownership in argenx.

Figure 1

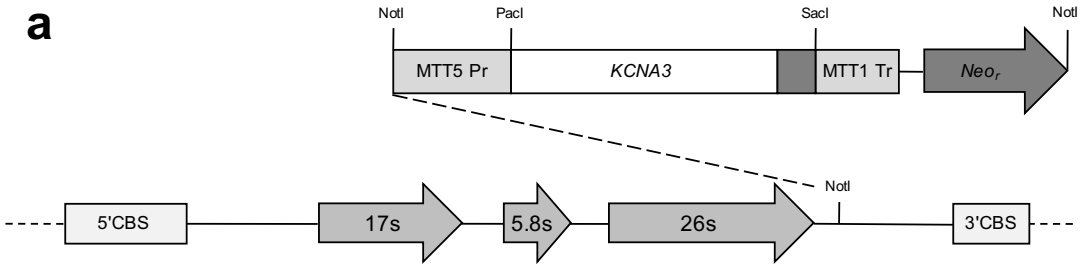
a
NotI
PacI
SacI
NotI
MTT5 Pr
KCNA3
MTT1 Tr
Neo$_r$
NotI
5'CBS
17s
5.8s
26s
3'CBS

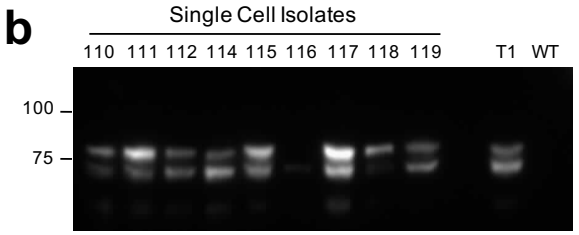
b
Single Cell Isolates
110 111 112 114 115 116 117 118 119
T1 WT
100
75

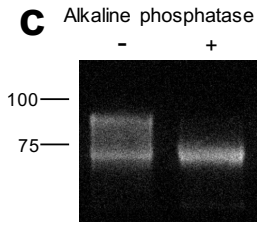
c
Alkaline phosphatase
-
+
100
75

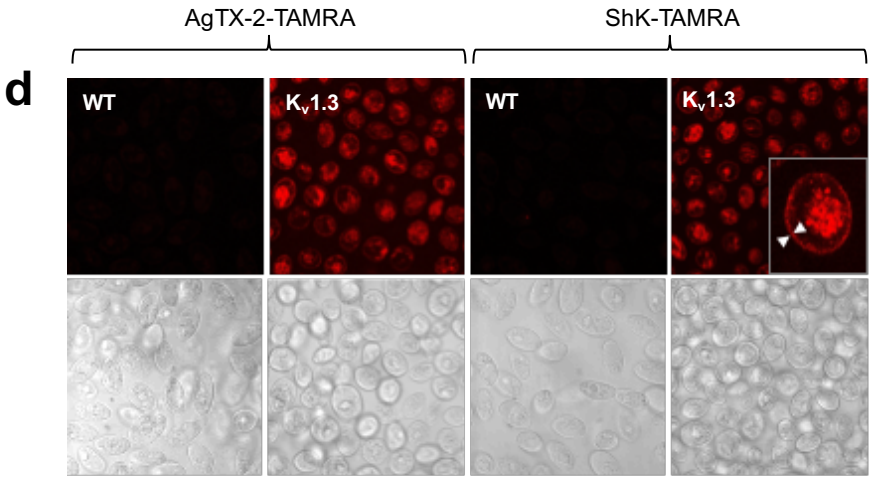
d
AgTX-2-TAMRA
ShK-TAMRA
WT
K$_v$1.3
WT
K$_v$1.3

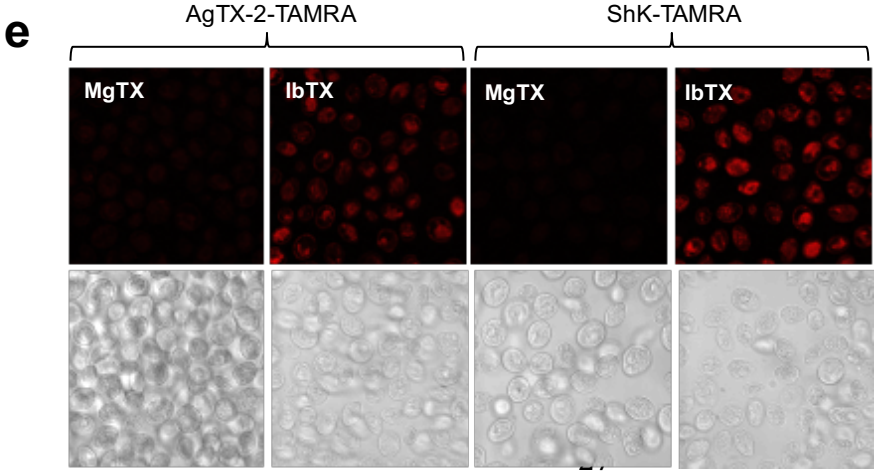
e
AgTX-2-TAMRA
ShK-TAMRA
MgTX
IbTX
MgTX
IbTX

Figure 2

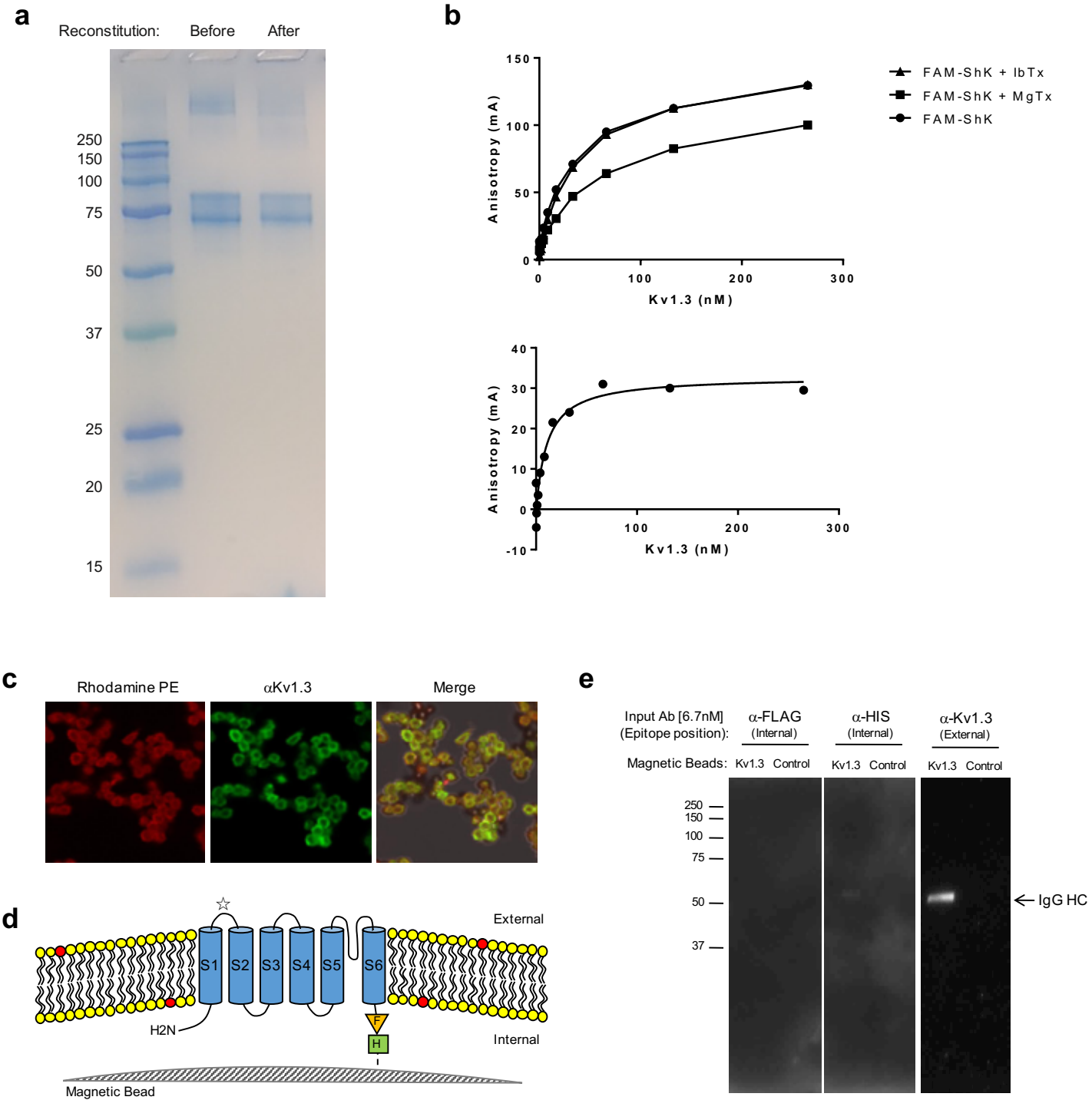
a
Reconstitution:
Before
After
250
150
100
75
50
37
25
20
15
b
Anisotropy (mA)
Kv1.3 (nM)
FAM-ShK + IbTx
FAM-ShK + MgTx
FAM-ShK
c
Rhodamine PE
αKv1.3
Merge
d
External
Internal
S1
S2
S3
S4
S5
S6
H2N
F
H
Magnetic Bead
e
Input Ab [6.7nM]
(Epitope position):
α-FLAG
(Internal)
α-HIS
(Internal)
α-Kv1.3
(External)
Magnetic Beads:
Kv1.3
Control
250
150
100
75
50
37
IgG HC

Figure 3

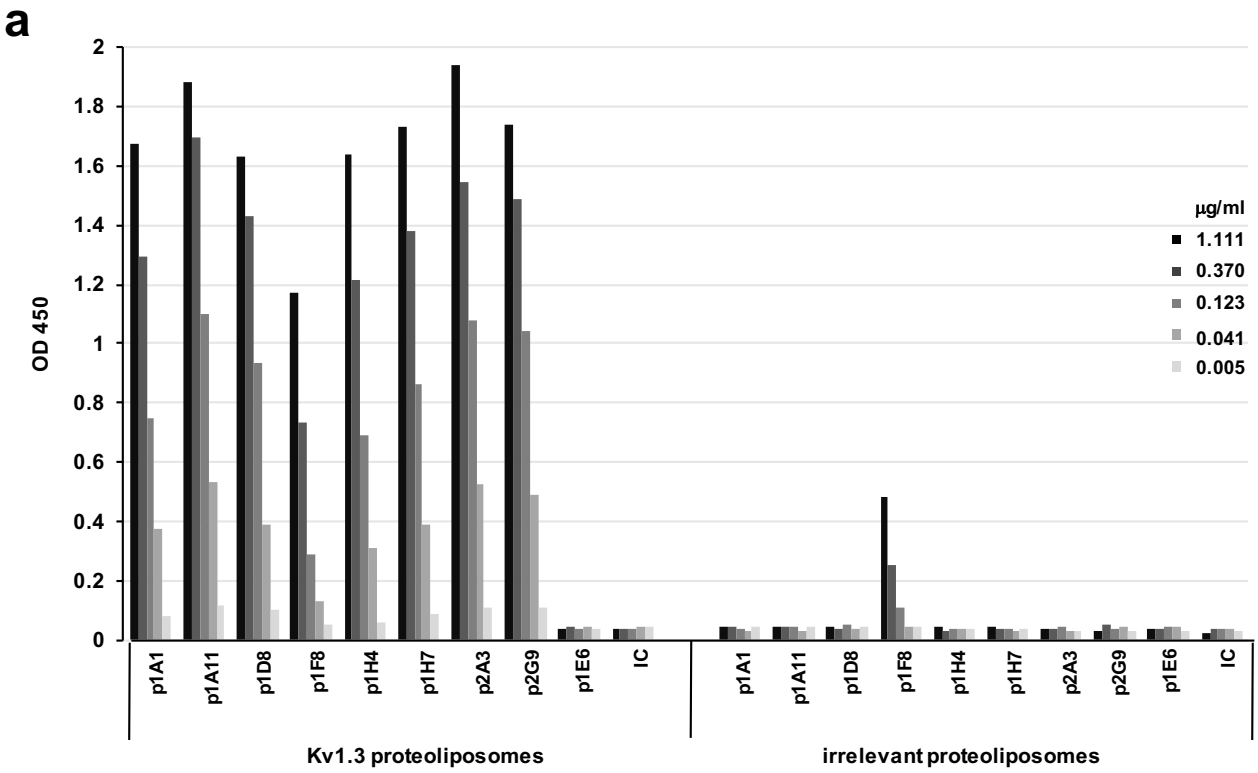
a
OD 450
2
1.8
1.6
1.4
1.2
1
0.8
0.6
0.4
0.2
0
µg/ml
1.111
0.370
0.123
0.041
0.005
p1A1
p1A11
p1D8
p1F8
p1H4
p1H7
p2A3
p2G9
p1E6
IC
Kv1.3 proteoliposomes
irrelevant proteoliposomes

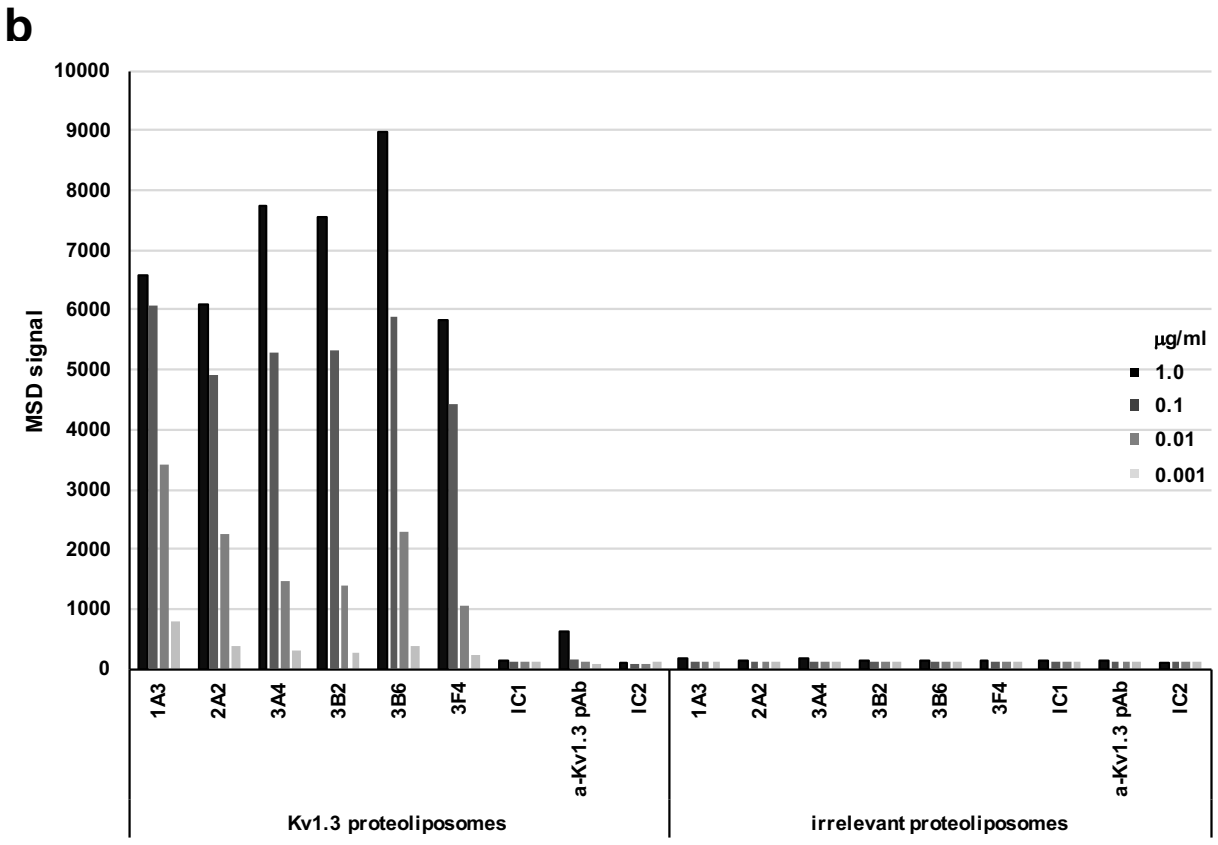
b
MSD signal
10000
9000
8000
7000
6000
5000
4000
3000
2000
1000
0
µg/ml
1.0
0.1
0.01
0.001
1A3
2A2
3A4
3B2
3B6
3F4
IC1
a-Kv1.3 pAb
IC2
Kv1.3 proteoliposomes
irrelevant proteoliposomes

Figure 4

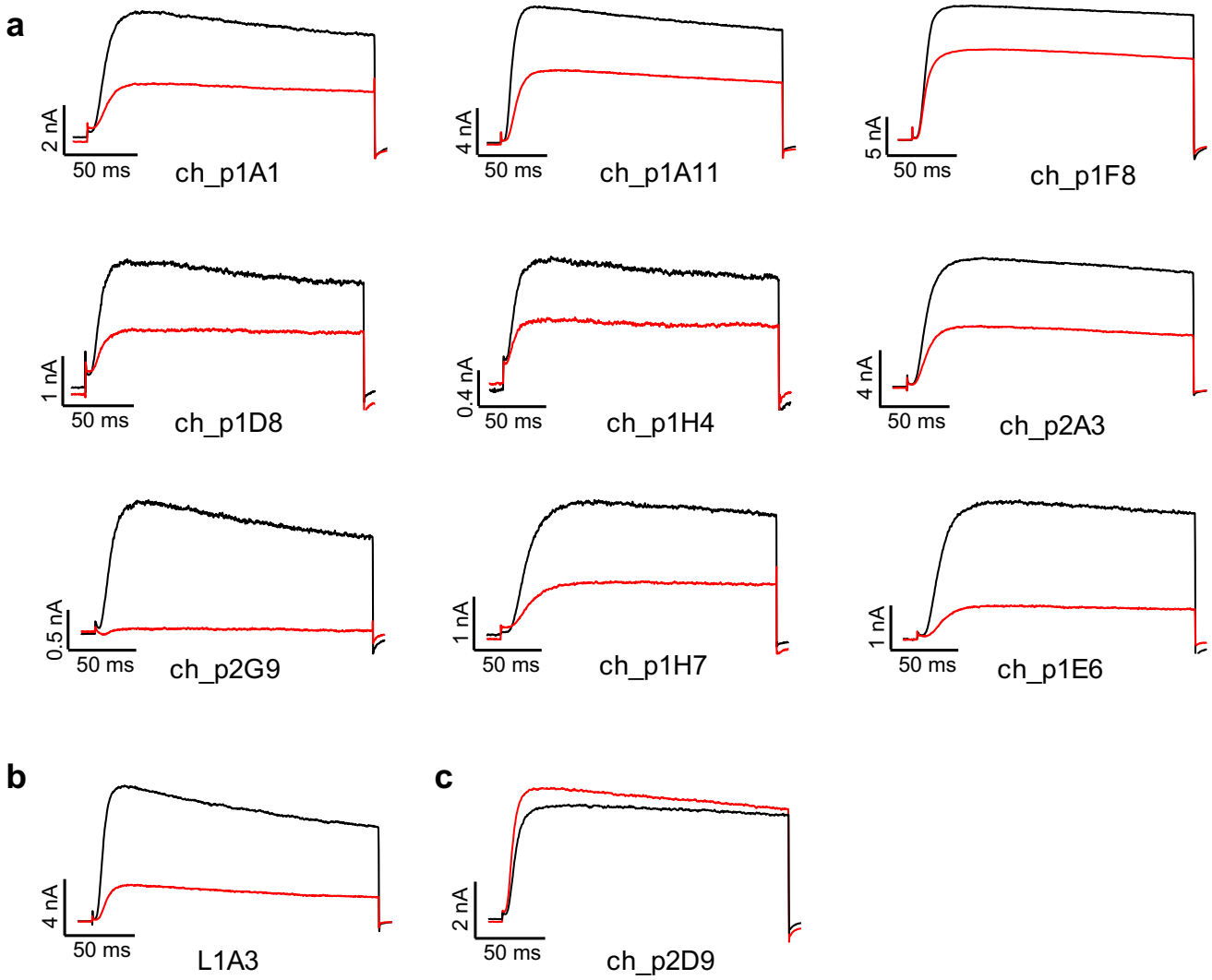
a
2 nA
50 ms
ch_p1A1
4 nA
50 ms
ch_p1A11
5 nA
50 ms
ch_p1F8
1 nA
50 ms
ch_p1D8
0.4 nA
50 ms
ch_p1H4
4 nA
50 ms
ch_p2A3
0.5 nA
50 ms
ch_p2G9
1 nA
50 ms
ch_p1H7
1 nA
50 ms
ch_p1E6
b
4 nA
50 ms
L1A3
c
2 nA
50 ms
ch_p2D9

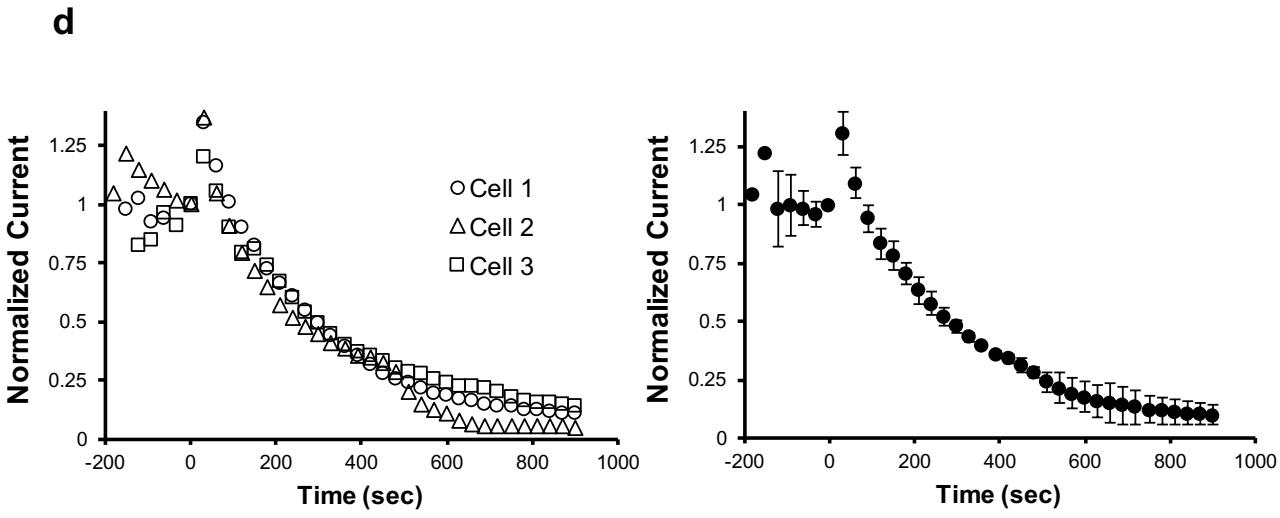
d
Normalized Current
1.25
1
0.75
0.5
0.25
0
-200
0
200
400
600
800
1000
Time (sec)
Cell 1
Cell 2
Cell 3
Normalized Current
Time (sec)

Figure 5

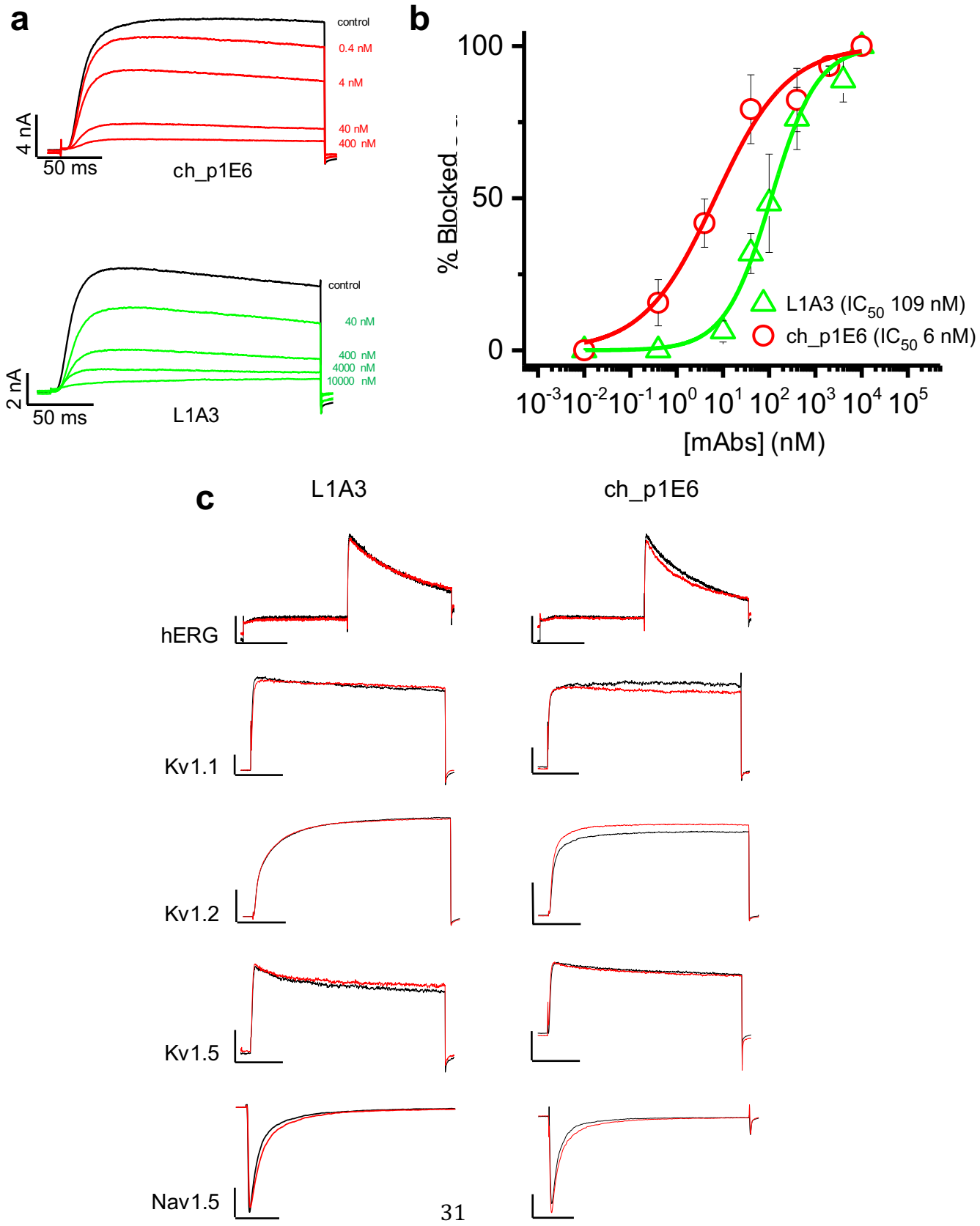
a
control
0.4 nM
4 nM
40 nM
400 nM
4 nA
50 ms
ch_p1E6
control
40 nM
400 nM
4000 nM
10000 nM
2 nA
50 ms
L1A3
b
100
50
0
% Blocked
L1A3 (IC50 109 nM)
ch_p1E6 (IC50 6 nM)
10-3 10-2 10-1 100 101 102 103 104 105
[mAbs] (nM)
c
L1A3
ch_p1E6
hERG
Kv1.1
Kv1.2
Kv1.5
Nav1.5

Figure 6

a

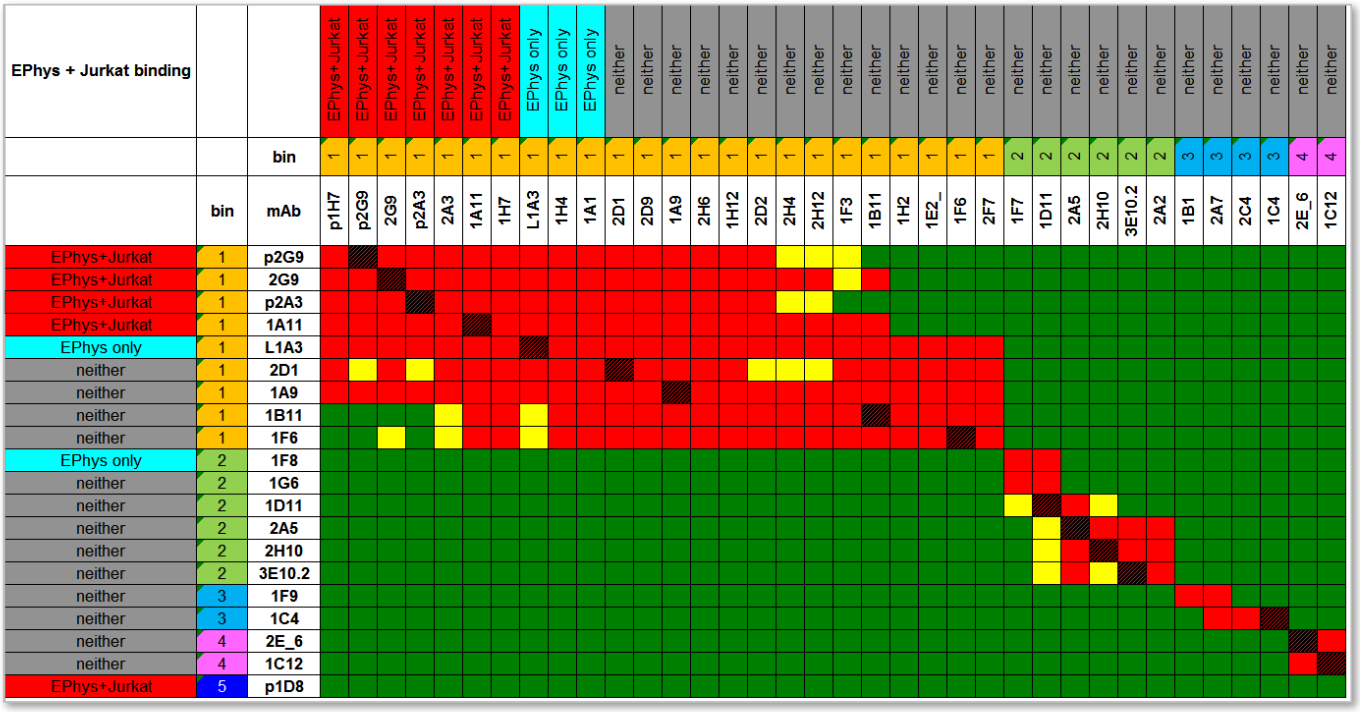
EPhys + Jurkat binding
bin
mAb
EPhys+Jurkat
EPhys only
neither
p1H7
p2G9
2G9
p2A3
2A3
1A11
1H7
L1A3
1H4
1A1
2D1
2D9
1A9
2H6
1H12
2D2
2H4
2H12
1F3
1B11
1H2
1E2_
1F6
2F7
1F7
1D11
2A5
2H10
3E10.2
2A2
1B1
2A7
2C4
1C4
2E_6
1C12
p1D8

b

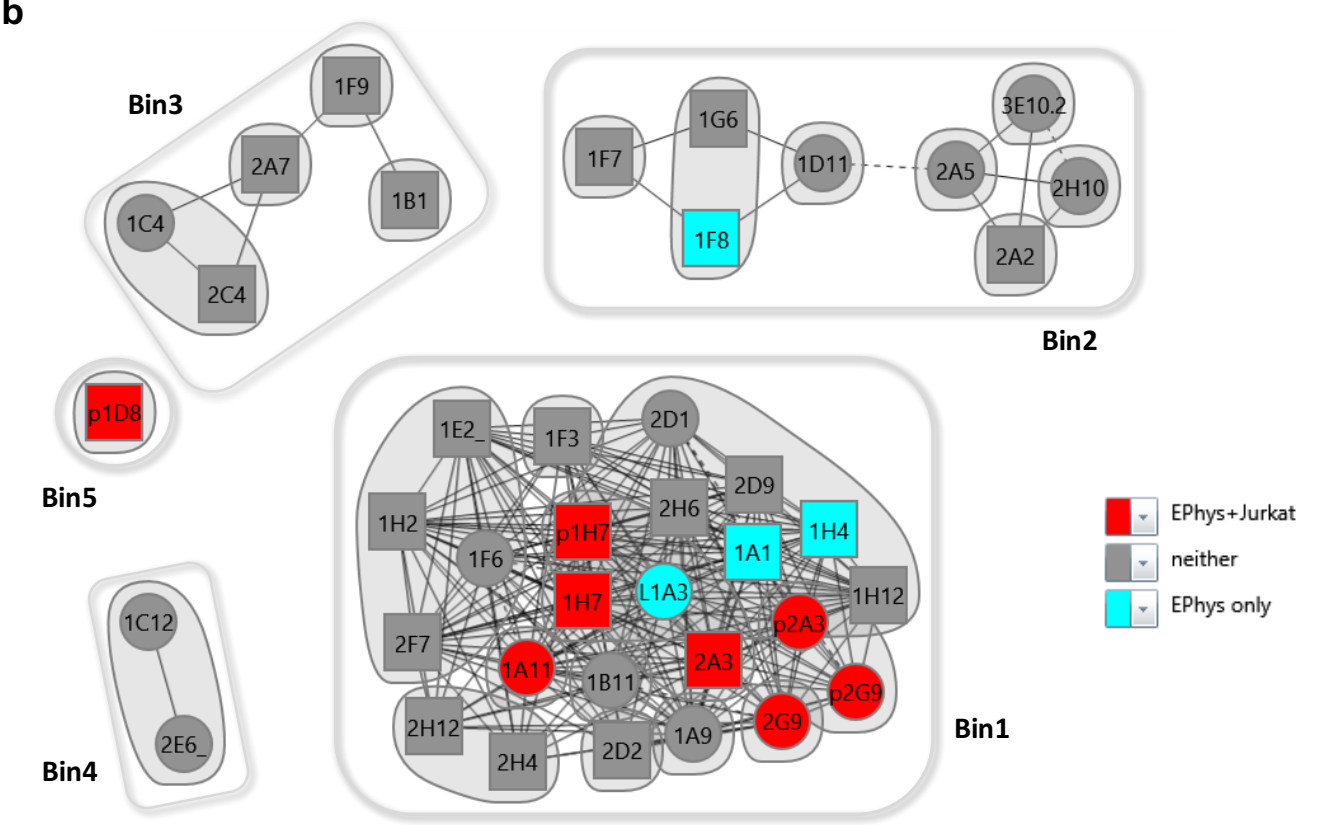
Bin3
1F9
2A7
1B1
1C4
2C4
Bin2
1G6
1F7
1D11
3E10.2
2A5
2H10
1F8
2A2
p1D8
Bin5
1E2_
1F3
2D1
2D9
1H2
2H6
1H4
p1H7
1A1
1F6
1H7
L1A3
1H12
p2A3
2F7
2A3
1A11
1B11
p2G9
2H12
2G9
1A9
2H4
2D2
Bin1
1C12
2E6_
Bin4
EPhys+Jurkat
neither
EPhys only

References

1. Eisen, J.A. *et al.* Macronuclear genome sequence of the ciliate Tetrahymena thermophila, a model eukaryote. *PLoS Biol.* **4**, e286 (2006).

2. Onimaru, H., Ohki, K., Nozawa, Y. & Naitoh Y. *Proc. Jpn. Acad.* Second edition, 538-543 (1980).

3. Hennessey, T.M & Kuruvilla, H.G. Electrophysiology of Tetrahymena. *Methods Cell Biol*. **62**, 363-377 (2000).

4. Wulff, H. *et al*. The voltage-gated Kv1.3 K^+ channel in effector memory T cells as a new target for MS. *J. Clin. Invest.* **111**, 1703-1713 (2003).

5. Beeton, C. *et al*. Kv1.3 channels are a therapeutic target for T cell-mediated autoimmune diseases. *Proc. Natl. Acad. Sci. USA* **103**, 17414-17419 (2006).

6. Rus, H. *et al*. The voltage-gated potassium channel Kv1.3 is highly expressed on inflammatory infiltrates in multiple sclerosis brain. *Proc. Natl. Acad. Sci. USA* **102**, 11094-11099 (2005).

7. Beeton, C. *et al*. Selective blockade of T lymphocyte K^+ channels ameliorates experimental autoimmune encephalomyelitis, a model for multiple sclerosis. *Proc. Natl. Acad. Sci. USA* **98**, 13942-13947 (2001).

8. Koo, G.C. *et al*. Blockade of the voltage-gated potassium channel Kv1.3 inhibits immune responses in vivo. *J. Immunol.* **158**, 5120-5128 (1997).

9. Matheu, M.P. *et al*. Imaging of effector memory T cells during a delayed-type hypersensitivity reaction and suppression by Kv1.3 channel block. *Immunity* **29**, 602-614 (2008).

10. Azam, P., Sankaranarayanan, A., Homerick, D., Griffey, S. & Wulff, H. Targeting effector memory T cells with the small molecule Kv1.3 blocker PAP-1 suppresses allergic contact dermatitis. *J. Invest. Dermatol.* **127**, 1419-1429 (2007).

11. Cheong, A. *et al*. Potent suppression of vascular smooth muscle cell migration and human neointimal hyperplasia by Kv1.3 channel blockers. *Cardiovasc. Res.* **89**, 282-289 (2011).

12. Hyodo, T. *et al*. Voltage-gated potassium channel blocker as a potential treatment for rat anti-glomerular basement membrane glomerulonephritis. *Am. J. Physiol*. **299**, 1258-1269 (2010).

13. Gilhar, A., Bergman, R., Assay, B., Ullmann, Y. & Etzioni, A. The beneficial effect of blocking Kv1.3 in the psoriasiform SCID mouse model. *J. Invest. Dermatol*. **131**, 118-124 (2011).

14. Gassmann, M., Thömmes, P., Wesier, T. & Hübsher, U. Efficient production of chicken egg yolk antibodies against a conserved mammalian protein. *FASEB J.* **4**, 2528-2532 (1990).

15. Klarenbeek, A. *et al*. Camelid Ig V genes reveal significant human homology not seen in therapeutic target genes, providing for a powerful therapeutic antibody platform. *mAbs* **7**, 693-706 (2015).

16. Diaz, S. *et al*. Tetrahymena Metallothioneins fall into two discrete subfamilies. *PLoS One* **3**, e291 (2007).

17. Blomberg, P., Randolph, C., Yao, C. H., & Yao, M.C. Regulatory sequences for the amplification and replication of the ribosomal DNA minichromosome in Tetrahymena thermophila. *Mol. Cell. Biol.* **17**, 7237-7247 (1997).

18. Holmes, T.C., Fadool D.A. & Levitan, I.B. Tyrosine phosphorylation of the Kv1.3 potassium channel. *J. Neurosci*. **16**, 1581-1590 (1996).

19. Garcia, M.L., Garcia-Calvo, M., Hidalgo, P., Lee, A. & MacKinnon, R. Purification and characterization of three inhibitors of voltage-dependent K+ channels from Leirus quinquestriatus var hebraeus venom. *Biochem*. **33**, 6834-6839 (1994).

20. Garcia-Calvo, M. *et al*. Purification, characterization, and biosynthesis of margatoxin, a component of Centruroides margaritatus venom that selectively inhibits voltage-dependent potassium channels. *J. Biol. Chem.* **268**, 18866-18874 (1993).

21. Pennington, M. et al. Chemical synthesis and characterization of ShK toxin: a potassium channel inhibitor from a sea anemone. *Int. J. Pept. Protein Res*. **346**, 354-358 (1995).

22. Aiyar, J. *et al*. Topology of the pore-region of a K+ channel revealed by the NMR-derived structures of scorpion toxins. *Neuron* **15**, 1169-1181 (1995).

23. Krezel, A.M., Kasibhatla, C., Hidalgo, P., MacKinnon, R. & Wagner, G. Solution structure of the potassium channel inhibitor agitoxin 2: Caliper for probing channel geometry. *Prot. Sci*. **4**, 1478-1489 (1995).

24. Helms, L.M.H. *et al*. Margatoxin binds to a homomultimer of Kv1.3 channels in Jurkat cells. Comparison with Kv1.3 expressed in CHO cells. *Biochem*. **36**, 3737-3744 (1997).

25. MacKinnon, R., Cohen, S.L., Kuo, A., Lee, A. & Chait, B.T. Structural conservation in prokaryotic and eukaryotic potassium channels. *Science* **280**, 106-109 (1998).

26. Valiyaveetil, F.I., Zhou, Y. & MacKinnon, R. Lipids in the structure, folding, and function of the KcsA K+ channel. *Biochemistry* **41**, 10771-10777 (2002).

27. Beeton, C. *et al*. A novel fluorescent toxin to detect and investigate Kv1.3 channel up-regulation in chronically activated T lymphocytes. *J. Biol. Chem*. **278**, 9928-9937 (2003).

28. Candia, S., Garcia, M.L. & Latorre, R. Mode of action of iberiotoxin, a potent blocker of the large conductance Ca^{2+}-activated K^+ channel. *Biophys. J*. **63**, 583-590 (1992).

29. Rossi, A.M. & Taylor, C.W. Analysis of protein-ligand interactions by fluorescence polarization. *Nature Protocols* **6**, 365-387 (2011).

30. Piper, D.R. *et al*. Development of the Predictor hERG fluorescence polarization assay using a membrane protein enrichment approach. *Assay and Drug Dev. Technol.* **6**, 213-223 (2008).

31. Jones, J.W. *et al*. Cell-free assay of G-protein-coupled receptors using fluorescence polarization. *J. Biomol. Screen* **13**, 424-429 (2008).

32. Dobrovinskaya, O. *et al.* Placing ion channel into a signaling network of T cells: from maturing thymocytes to healthy T lymphocytes or leukemic T lymphoblasts. *Biomed. Res. Int.* 2015, 750203 (2015).

33. Yang, X-F. *et al*. The antibody targeting the E314 peptide of human Kv1.3 pore region serves as a novel, potent and specific channel blocker. *PLoS One* **7**, e36379 (2012).

34. Wang, R.E. *et al*. Rational design of a Kv1.3 channel-blocking antibody as a selective immunosuppressant. *Proc. Natl. Acad. Sci. USA* **113**, 11501-11506 (2016).

35. O Starkie, D., Compson, J.E., Rapecki, S. & Lightwood, D.J. Generation of recombinant monoclonal antibodies from immunized mice and rabbits via flow cytometry and sorting of antigen-specific IgG^+ memory B cells*. PLoS One* **11**, e0152282 (2016).

36.Tarcha, E.J. *et al.* Safety and pharmacodynamics of dalazatide, a Kv1.3 channel inhibitor, in the treatment of plaque psoriasis: a randomized phase 1b trial. *PLoS One* **12**, e0180762 (2017).

37. Cassidy-Hanley, D. *et al*. Germline and somatic transformation of mating Tetrahymena thermophila by particle bombardment. *Genetics* **146**, 135-147 (1997).

38. Izquierdo S.M. *et al*. High-efficiency antibody discovery achieved with multiplexed microscopy. *Microscopy* **65**, 341-352 (2016).

39. van der Woning, B. *et al*. DNA immunization combined with scFv phage display identifies antagonistic GCGR specific antibodies and reveals new epitopes on the small extracellular loops. *mAbs* **8**, 1126-35 (2016).

40. Basilico, C. *et al*. Four individually druggable MET hotspots mediate HGF-driven tumor progression. *J. Clin. Invest.* **124**, 3712-3786 (2014).

41. de Haard, H.J. *et al*. A large non-immunized human Fab fragment phage library that permits rapid isolation and kinetic analysis of high affinity antibodies. *J. Biol. Chem.* **274**, 18218-18230 (1999).

42. Barbas, C.F. 3rd *et al*. Recombinant human Fab fragments neutralize human type 1 immunodeficiency virus in vitro. *Proc. Natl. Acad. Sci. USA* **89**, 9339-9343 (1992).

43. Coleman, N. *et al*. New positive Ca2+-activated K+ channel gating modulators with selectivity for KCa3.1. *Mol. Pharmacol*. **86**, 342-357 (2014).

44. Schmitz, A. *et al*. Design of PAP-1, a selective small molecule Kv1.3 blocker, for the suppression of effector memory T cells in autoimmune diseases. *Mol. Pharmacol*. **68**, 1254-1270 (2005).

45. Abdiche, Y.N. *et al*. High-throughput epitope binning assays on label-free array-based biosensors can yield exquisite epitope discrimination that facilitates the selection of monoclonal antibodies with functional activity. *PLoS One* **9**, e92451 (2014).

FIGURE LEGENDS

Figure 1. Expression of human Kv1.3 in *Tetrahymena thermophila*. a. Expression construct design. *KCNA3*, the gene encoding human Kv1.3, was modified with a C-terminal FLAG/10XHis tag and placed under the control of the MTT5 and MTT1 promoter and terminator, respectively. The entire expression cassette was cloned as a NotI fragment into an rDNA vector, pTRAS1. The relative positions of chromosome breakage sites (CBS) and ribosomal genes (17s, 5.8s, and 26s) are shown. **b. Single cell isolates maintain expression of recombinant Kv1.3.** Anti-Kv1.3 Western analysis of single cells isolated from pooled *Tetrahymena* transformants and tested for their ability to express Kv1.3. Eight of nine single cell isolates expressed Kv1.3 at similar levels to the original pool (T1) with one clone (#117) expressing higher-levels of Kv1.3. A lysate from wild-type cells (WT) was included as a negative control. **c. *Tetrahymena*-expressed Kv1.3 is phosphorylated.** Purified Kv1.3 was incubated in the absence (-) and presence (+) of calf-intestinal alkaline phosphatase (CIP) and subsequently detected by anti-Kv1.3 Western analysis as described above. **d. *Tetrahymena*-expressed Kv1.3 binds both Agitoxin-2 (AgTX-2) and ShK.** Mock-induced wild-type cells (WT) and Kv1.3-expressing *Tetrahymena* cells were fixed and labeled with either 10 nM Agitoxin-2-TAMRA (AgTX-2-TAMRA) or ShK-TAMRA and visualized by fluorescence confocal microscopy. Inset shows a close-image of a single *Tetrahymena* cell. White arrows highlight the *Tetrahymena* plasma (surface) membrane. **e. Binding of ShK to *Tetrahymena* Kv1.3 is specific.** Fixed *Tetrahymena* cells expressing Kv1.3 were incubated with 10 nM ShK-TAMRA in the presence of saturating (10X) amounts of Margatoxin (MgTx) or Iberiotoxin (IbTx) and examined by fluorescence confocal microscopy.

Figure 2. Purification of recombinant Kv1.3. a. SDS-PAGE analysis of purified and reconstituted Kv1.3. Kv1.3 was purified as described in Materials, resolved by SDS-PAGE before and after reconstitution into liposomes and stained with SimplyBlue™ SafeStain™. **b.**

Ligand Binding Analysis. Kv1.3-containing liposomes were incubated with FAM-ShK (3 nM) in the presence or absence of a 50-fold excess of either MgTx or IbTx. Top Panel is a representative experiment showing total binding expressed as Anisotropy measured by fluorescence polarization. Bottom Panel represents specific binding to FAM-ShK. Kd was estimated as 11.5 nM +/- 3.4 nM based on specific binding curves generated in three separate experiments **c. Fluorescence microscopy analysis of Kv1.3 magnetic beads.** Magnetic beads containing tethered Kv1.3 reconstituted into a lipid bilayer consisting of rhodamine-labeled PE and non-labeled PC were examined by fluorescence microscopy. Beads were examined under a rhodamine filter to detect labeled PE incorporation (Left Panel) and with a FITC-filter following labelling with an anti-Kv1.3 antibody that recognizes an epitope on the first extracellular loop and anti-guinea pig conjugated FITC (Middle Panel). Rhodamine and FITC-images were merged (Right Panel) to confirm co-localization of Kv1.3 and the lipid bilayer (yellow fluorescence). **d. Schematic illustration of Kv1.3 magnetic beads.** Shown is the magnetic bead surface; the lipid bilayer consisting of PC (yellow lipids) and Rhodamine-labeled PE (red lipids); the six transmembrane domains of the Kv1.3 monomer (S1-S6); the C-terminal engineered FLAG (orange Triangle) and 10XHis (Green Box) tags; a star indicates the position of the epitope on the first extracellular loop that is recognized by the Kv1.3 antibody utilized in c and d. **e. Kv1.3 magnetic beads preferentially pull-down an antibody that recognizes an extracellular epitope.** Kv1.3 magnetic beads or control beads were incubated with antibodies (6.7 nM) that recognize either internal (FLAG and 10XHis) or external (Kv1.3) epitopes. Beads were washed and bound IgG eluted directly in SDS-PAGE loading buffer. IgG was detected by Western analysis using either anti-mouse-HRP (anti-FLAG and -His) or anti-guinea pig-HRP (anti-Kv1.3).

Figure 3. Identification of anti-Kv1.3 antibodies. a. Chicken anti-Kv1.3 antibodies. ScFv-Fc screening was carried out by ELISA using three-fold serial dilutions of antibody against

proteoliposomes containing Kv1.3 or an irrelevant human VGIC also expressed in *Tetrahymena*. An isotype control (IC) for generated antibodies was also included. Shown are results for antibodies that inhibit Kv1.3 activity. Note the relative lack of reactivity of clone ch_p1E6 against Kv1.3 and clone p1F8 reactivity against the irrelevant proteoliposome control. **b. Llama anti-Kv1.3 antibodies.** ScFv-Fc screening was carried out using ten-fold serial dilutions of antibody on mesoscale against proteoliposomes containing Kv1.3 or an irrelevant human VGIC also expressed in *Tetrahymena*. IC1, isotype control for generated antibodies; IC2, isotype control for anti-Kv1.3 polyclonal antibody. Data is shown for 6 out of 19 specific Kv1.3 binding scFv-Fc antibodies.

Figure 4. Identification of anti-Kv1.3 antibodies that functionally inhibit Kv1.3 channel activity. Purified scFv-Fc anti-Kv1.3 antibodies from either chickens or llamas were tested at a concentration of 400nM via electrophysiology for their ability to block current from human Kv1.3 expressed in L929 fibroblast cells. Shown are representative traces for each of the antibodies that blocked Kv1.3 current. Black lines represent control currents, red lines represent currents following addition of antibody. Inhibiting anti-Kv1.3 antibody clones derived from chickens are shown in a, the functional llama anti-Kv1.3 antibody is shown in b. An example of an antibody that was tested and shown not to modulate Kv1.3 activity is shown in c. **d. Time-dependent development of current inhibition by monoclonal antibodies targeting Kv1.3.** (Left Panel) Time-current plots showing current inhibition of three (3) individual cells expressing hKv1.3 channels by the monoclonal antibody ScFv-Fc L1A3. Antibodies were added after current stabilization at 0 second. Currents were elicited by pulsing to +40 mV for 200 ms from a holding potential of -80 mV every 30 seconds. (Right Panel) Means ± SD plot of the current inhibition of three individual cells in the left panel. Similar time-dependent profiles were observed for each of the blocking antibodies.

Figure 5. Anti-Kv1.3 antibody potency analysis. a. Dose response curves. Ten-fold serial dilutions of chicken antibody p1E6 (red traces) and llama antibody L1A3 (green traces) were used to generate dose-response curves. Black lines represent control currents. **b. IC_{50} Determinations.** IC_{50}s for p1E6 (red curve) and L1A3 (green curve) were determined by fitting the calculated percentage of current block to a Hill equation. IC_{50}s for p1E6 and L1A3 were estimated as 6 and 109 nM, respectively **c**. **Analysis of p1E6 and L1A3 selectivity.** ScFv-Fc clones p1E6 and L1A3 were tested for their ability to block the activity of related Kv1.x family members (Kv1.1, Kv1.2, Kv1.5), hERG and Nav1.5 at a concentration of 1 μM. Shown are representative traces from each experiment. Black lines, control current; Red lines, currents following addition of antibody.

Figure 6. Kv1.3 epitope binning analysis. a. Binning analysis heat map. Shown are antibodies colored by bin (1-5) and by functional data. Antibodies that block Kv1.3 current are highlighted in blue (Ephys only), those that additionally bind Jurkat cells are highlighted in red (Ephys + Jurkat) and those that do neither are highlighted in grey. Relative competition activity of each antibody is color coded and indicates strong competition (red boxes), intermediate/weak competition (yellow boxes) or no competition (green boxes). Dark red boxes indicate competition from the same antibody pair. **b. Binning network plot.** Antibodies are colored to identify those that inhibit channel activity (blue), additionally bind Jurkat cells (red) or do neither (grey). Note antibody L1A3 was not tested for its ability to bind Jurkat cells, however, for simplicity was denoted as inhibiting ion channel only (blue) in **a** & **b**.

Table 1. Summary of anti-Kv1.3 antibody identification

Antibody Platform	Screening Method	ELISA positive (unique sequences)	Functional Antibodies Identified
Chicken	GEM Assay: Kv1.3 Proteoliposomes	25	7
	GEM Assay: Kv1.3 Magnetic Beads	16	2
	GEM Assay: Kv1.3 Whole Cells	10	0
Llama	Phage Display: Kv1.3 Magnetic Beads	19	1
	Total	**70**	10

Table 2. Summary of anti-Kv1.3 antibody functional activity

	Percent Kv1.3 current blocked at 400 nM		
scFv-Fc clone	Average block (%)	STDEV (%)	*n*
ch_p1A1	50.28	13.02	8
ch_p1A11	56.51	10.1	6
ch_p1F8	44.34	12.12	3
ch_p1D8	54.47	1.52	3
ch_p1H4	45.99	12.38	6
ch_p2A3	45.02	3.5	2
ch_p2G9	75.35	11.65	11
ch_p1H7	47.32	12.42	2
ch_p1E6	82.28	10.45	12
L1A3	73.53	8.71	3

Table 3. L1A3 and p1E6 selectivity profile

Channels	L1A3		p1E6	
	% Blocked at 1 µM (Mean ± SD)	n	% Blocked at 1 µM (Mean ± SD)	n
Kv1.1	4.18 ± 2.65	2	3.87 ± 2.65	2
Kv1.2	0.68 ± 0.97	2	0.00 ± 0.00	2
Kv1.5	0.48 ± 0.69	2	1.28 ± 1.80	2
Kv11.1 (hERG)	2.11 ± 2.98	2	5.32 ± 0.45	2
Nav1.5	4.98 ± 3.09	3	0.00 ± 0.00	2

Table 4. Kv1.3 ortholog sequence alignment analysis

	Percent Identity (CLUTSAL Omega)		
Query: *H. sapiens*	***M. Musculus (mouse)***	***G. gallus (chicken)***	***V. pacos (llama)***
P22001.3	**NP_032444.2**	**AAP94028.1**	**XP_006197566**
full-length	97.51	83.15	97.72
S1-S2 ECD	85.71	52.5	80.95
S3-S4 ECD	100	100	100
S5-S6 ECD/Pore	94.74	94.74	100